Liquid crystalline behavior of octylcyanobiphenyl confined to submicron-size randomly connected porous glasses

Germano S. Iannacchione,* Sihai Qian, and Daniele Finotello
Department of Physics and Liquid Crystal Institute, Kent State University, Kent, Ohio 44242

Fouad M. Aliev
Department of Physics, University of Puerto Rico, San Juan, Puerto Rico 00931
(Received 7 February 1997)

We report a study of the orientational order via deuterium NMR and high resolution ac calorimetry on octylcyanobiphenyl (8CB) confined to randomly oriented and interconnected macroporous (1000 Å mean pore size) and microporous (100 Å mean pore size) glasses. In the macroporous glass, the nematic to isotropic (N-I) phase transition retains the bulklike weakly first order nature. The nematic phase is characterized by an NMR powder pattern spectra, as expected for a director distribution with no preferred spatial direction, and it coexists with an isotropiclike component. The orientational order is slightly suppressed from the bulk's and there is no sudden increase in orientational order due to the onset of the smectic phase suggesting a weaker coupling between nematic and smectic order parameters. Further, due to the confining size, the smectic-A to nematic transition is considerably suppressed and broadened. In the microporous glass, the orientational order behavior is reminiscent of that in Vycor glass. No phase transitions are detected, rather, there is a continuous evolution of local orientational order. Interporous and intraporous interactions are important.
[S1063-651X(97)02507-5]

PACS number(s): 61.30.−v, 65.20.+w, 76.60.−k

I. INTRODUCTION

The study of physical systems confined to a random network of pores is a particularly rich area of research. Fundamental questions of how phase structure and transitions are modified in a confining environment remain open issues. Complex fluids confined to randomly interconnected porous networks are unique systems in that they allow us to address such questions. Historically, aside from the extensive research at the confined superfluid transition [1], the first complex fluid system to be studied confined to a random porous media were binary liquid mixtures (BLM) where experimental evidence [2,3] suggested that a ''random-field'' model [4–6] can describe the modifications occurring at phase transitions.

In the first photon correlation spectroscopy experiments with liquid crystals (LC) impregnating a random porous media [7], it was shown that a random-field approach can also be applied to interpret the dynamics of nematic ordering. There, the nematic phase within the pores was modeled as an Ising-like system which was developed for magnetic spins, with an imposed random uniaxial field coupled directly to the orientational order parameter (S) to account for the random confinement. The model uses a random uniaxial anisotropy on a spin system [8–10] (as in Refs. [4–6]) including a symmetric coupling between the anisotropy vector and S in order to account for the ''up-down'' symmetry of the nematic director. Such models may be described as random-field Ising models (RFI). At phase transitions, recent computer simulations find a specific heat peak at the N-I transition shifted to lower temperatures and considerably broadened, with no evidence of the bulk's first order nature [10]. For sufficiently restrictive hosts (e.g., pore sizes smaller than the ~150 Å thermal nematic correlation length), the models predict the replacement of the first order N-I transition by a continuous transition to a glassylike state in agreement with experimental results [10].

Recent studies indicate that RFI models may be applicable only when macroscopic order is still possible, i.e., confinements where large interpore interactions are dominant [11–17]. Experimental observations for BLM systems that can be interpreted by a RFI model, may also be described by phase wetting where the confinement inhibits ordered phase domain growth [18–20]. An obvious difficulty of these static models is that they do not account for the extremely slow dynamics (long relaxation times) which are observed for order parameter fluctuations [12–14]. Confining geometries where the pore structure minimizes the pore-to-pore interactions cannot be expected to follow the RFI model predictions [21–26]. In such cases, an appropriate approach is a single-pore (SP) model which considers ordering within a single, independent, pore. This is then averaged with a suitable distribution that describes the confining host, over the entire sample [23,24]. RFI type of models are further improved when local correlations are taken into account.

In this work we report on a study for a octylcyanobiphenyl (8CB) liquid crystal confined to two sintered porous glasses: a 1000 Å mean pore size (macroporous) and a 100 Å mean pore size (microporous) glass. Deuterium NMR (DNMR) spectroscopy and high resolution ac calorimetry probed the orientational order and the thermodynamics of the two bulk phase transitions, namely, the weakly first order N-I and the second order smectic-A to nematic (Sm-A–N)

*Present address: Center for Material Science and Engineering, MIT, Cambridge, MA 02154.

transitions, within both porous materials. Under microporous confinement, there is no evidence for a phase transition to a nematic phase from high temperature isotropic-fluid phase. Instead, there appears a gradual evolution of local orientational ordering which continuously increases with decreasing temperature. This agrees with the behavior observed for LC confined to Vycor glass, a 70 Å size, interconnected, porous media [24]. Those results were well understood via a SP model where the orientational order is mostly dominated by the local environment. In the macroporous confinement, a bulklike N-I transition is retained as determined by both DNMR and calorimetry. Below the transition temperature T_{NI} determined by DNMR, the orientational order increases with a temperature dependence different from bulk's until $\sim$2.3 K below T_{NI} where the growth exhibits an identical temperature dependence to that of bulk. At lower temperatures, the sudden enhancement in orientational order, which characterizes the bulk Sm-$A-N$ transition, is absent. This suggests a confinement induced decoupling of the smectic and nematic order parameters.

This paper, mostly focuses on the N-I transition and to a lesser extent, on the confined Sm-$A-N$ transitions, and their differences with respect to bulk, is organized as follows. A brief overview on the experimental techniques employed and the sample preparations is presented in Sec. II. In Sec. III, the experimental results for 8CB confined to the macroporous and microporous glasses are presented. We conclude by summarizing the results and discussing their implications on other confinement studies.

II. EXPERIMENTAL TECHNIQUES

The sintered porous glasses used in this work are fabricated in a similar manner to Vycor ''thirsty'' glass [27,28]; i.e., a spinodal decomposition of a mixture of SiO_2 and BrO_2. The boron oxide rich phase is then etched away in an acid bath leaving a pure network of fired SiO_2 glass. The confining topology can be described as a network of three-dimensional (3D) randomly connected pore segments uniformly distributed in orientation and density. The 25% porosity microporous glass has a mean pore diameter of $d \sim 100$ Å, a surface to open volume ratio of 0.01 $Å^{-1}$ and the density is 1.65 g/cm^3. The 40% porosity macroporous glass has a mean pore diameter $d \sim 1000$ Å, a surface to open volume ratio of 0.0016 $Å^{-1}$, and a density of 1.32 g/cm^3.

Bulk 8CB, which for the DNMR experiments was deuterated in the first carbon position along the alkyl chain from the biphenyl rings, exhibits a weakly first order N-I transition at 314.02 K, a second order Sm-$A-N$ transition at 307.02 K, and a strongly first order crystallization (crystal–Sm-A) transition near 295 K. The bulk enthalpies (δH) and latent heats (l) for these transitions are $\delta H_{NI}=2.13$ J/g and $l_{NI}=2.10$ J/g, $\delta H_{\text{Sm-}A-N}=0.48$ J/g and $l_{\text{Sm-}A-\text{N}}=0.001\,37$ J/g, and $l_{\text{crystal-Sm-}A}=97.1$ J/g, respectively [29].

A. Deuterium nuclear magnetic resonance

Nuclear magnetic resonance is an extremely valuable tool in liquid crystal studies as it probes the orientational order, director configurations, and molecular dynamics. Deuterium NMR has been extensively and successfully applied to the study of bulk [30] and, more recently, to confined liquid crystals [31].

Our spectrometer consists of a 4.7 T (200 MHz for protons, 30.8 MHz for deuterium) superconducting magnet fitted with a homemade probe and electronics. The probe head is inserted in an oven housed in the magnet bore, through which a mixture of ethylene glycohol and water circulates from an external temperature controlled bath. The probe head is provided with a calibrated 100 Ω platinum thermometer which is read after each DNMR pulse sequence and averaged over the accumulated scans. The temperature stability over the entire DNMR spectra acquisition time is better than ± 0.05 K with a resolution of ± 0.005 K.

The DNMR samples consist of a cylinder of the desired porous glass, $\sim$5 mm in diameter and 15 mm long, filled with deuterated 8 CB (α deuterated). Prior to imbedding the liquid crystal, the glass was cleaned by boiling it in a 30% solution of hydrogen peroxide–distilled water bath, and ultrasonically agitated for several hours before drying under vacuum at $\sim$100 °C. The glass piece was then immediately placed and left overnight in an isotropic bath of 8CB. While in the isotropic phase, the sample was wiped with Whatman absorbent filter paper to remove excess liquid crystals from the outer glass surface. Measurements were performed, both heating and cooling, after thermally cycling the sample several times about the bulk N-I transition in the presence of the DNMR field.

Measurements used a quadrupole-echo pulse sequence ($90°_x$-τ-$90°_y$-τ acquisition) with full phase cycling: $\tau \cong 100$ μs, $90° \cong 3$ μs, a 1024–2048 point acquisition, and a last delay of 300 ms (which prevents T_1 saturation). This sequence was accumulated for up to 50 000 scans over a 2 h period. The final spectra is obtained by a complex Fourier transform of the single zero-filled free induction decay. In the nematic phase, the presence of orientational order splits the quadrupolar resonance line by [30,32]

$$\delta\nu = \tfrac{1}{2}\delta\nu_0 S(3\cos^2\theta_B - 1), \tag{1}$$

where $\delta\nu_0$ is the maximum possible splitting observable for completely aligned bulk nematic sample, S is the scalar order parameter, and θ_B is the angle that the nematic director (n) makes with the static NMR field ($\mathbf{B}_0$). For bulk, $\theta_B = 0°$ due to the uniform $\mathbf{B}_0$ field alignment of $\mathbf{n}$. For sufficiently confined liquid crystals, the splitting has a positional dependence, $\delta\nu = \delta\nu(\mathbf{r})$, through some director structure $\theta_B = \theta_B(\mathbf{r})$. Equation (1) thus becomes [31–33]

$$\delta\nu(\mathbf{r}) = \tfrac{1}{2}\delta\nu_0[S(\mathbf{r})/S_0][3\cos^2\theta_B(\mathbf{r}) - 1], \tag{2}$$

where S_0 is the bulk nematic order. The observed spectra result from $\delta\nu(r)$ averaged over all r in the sample. For a director structure unaffected by the field $\mathbf{B}_0$, the confining length, l (i.e., pore size), must be smaller than the magnetic coherence length, which for our magnet is $\xi_M \approx 1$ μm for 8CB [31–33].

For a typical bulk liquid crystal sample, the DNMR spectral pattern consists of two sharp absorption lines, typically 200–400 Hz full width half maximum (FWHM), separated by an amount $\delta\nu_{\text{bulk}} = \delta\nu_0 S_0$, the quadrupolar splitting. For a confined sample with a single scalar order parameter S

(often smaller than bulk's) but with an isotropic angular distribution in the nematic director orientation, a powder pattern is observed [30]. For instance, for a spherical distribution of the director, shoulders with a splitting equal to $\delta\nu_{\text{bulk}}$, and 90° singularities with a splitting $1/2\delta\nu_{\text{bulk}}$ for the same scalar order parameter would be seen [31]. A spherical distribution represents the most isotropic distribution possible. If a distribution in the scalar order parameter not centered at $S=0$ also exists, then, a superposition of spherical powder patterns is observed having the same distribution. The FWHM of this pattern would be $\delta\nu_{1/2}=\frac{1}{2}\delta\nu_0 S$. If this distribution in S is narrow and centered at $S=0$, then, a single sharp Lorentzian absorption peak with FWHM~50 Hz would be observed as for isotropic bulk liquid crystals.

The above description does not consider the presence of defects, small regions ~10 nm in diameter having $S\approx 0$, nor the effects of motional diffusional averaging. The extent of motional averaging can be estimated from $x_0\approx(D/\delta\nu)^{1/2}$ [32], where D is the diffusion constant and x_0 the distance molecules migrate during the time of a DNMR experiment. It should be noted that under certain confinement conditions, diffusion may be inhibited except for a thin layer in contact with the solid substrate. However, for local averaging over a single pore, the diffusion constant can be taken to be that of bulk LC. Using typical nematic phase values for nCB, $x_0 \approx 0.02\ \mu$m, while in the isotropic phase it is an order of magnitude larger, $x_0\approx 0.2\ \mu$m [24,34]. Thus, if $S(r)$ is nearly constant over the confining void, the DNMR spectra reflects the true static director structure. If $S(r)$ varies considerably, as in the case of defects spaced closer than x_0, then, the DNMR spectra will include considerable motional averaging resulting in the narrowing of all features.

B. ac calorimetry

ac calorimetry [35] is an extremely sensitive technique that permits an accurate measurement of the heat capacity of small samples near phase transitions. The technique has been employed in precise measurements at the phase transitions of bulk [36] and confined [37] liquid crystals. Our implementation of the ac technique for liquid crystal research, as well as to two-dimensional helium films, has already appeared in the literature [38] and only a brief review is included here.

Measurements take place under near equilibrium conditions as the sample is set into very small temperature oscillations about a precisely determined average temperature. The amplitude of the resulting temperature oscillations is inversely proportional to the heat capacity C of the sample. This amplitude, T_{ac}, can be written as [35,38]

$$T_{\text{ac}}=(Q_0/2\omega C)[1+(\omega\tau_i)^2+(1/\omega\tau_e)^2]^{-1/2}, \qquad (3)$$

where the thermal relaxation times are defined as $\tau_e = C/K_b$ (external) and $\tau_1^2=\tau_\theta^2+\tau_h^2+\tau_s^2$ (internal). The individual relaxation times are $\tau_\theta=C_\theta/K_\theta$, $\tau_h=C_h/K_h$, and $\tau_s=C_S/K_S$ corresponding to the thermometer, heater, and sample, respectively. The internal time constant is the time required for the entire assembly to reach equilibrium with the applied heat while the external time constant is the time required to achieve equilibrium with the surrounding bath.

The calorimeter has an internal time constant of approximately 1.26 s (0.79 Hz high frequency roll off) and an external time constant of about 31.4 s (0.032 Hz low frequency roll off). The addendum heat capacity is 42 mJ/K at 303 K, increasing linearly with temperature at a rate of 0.286 mJ/K^2. The applied voltage frequency was 55 mHz and the induced temperature oscillations were ~2 mK peak to peak. Data, spaced at roughly 10 mK intervals, is averaged for 8 to 10 min at every temperature.

The samples for the specific heat studies consisted of a small piece of the porous glass, $\sim 7\times 3$ mm, which was shaved to <0.5 mm thick. They each weighted ~11 mg and contained roughly 2.5 mg of 8 CB from the same LC batch used for the DNMR measurements. Cleaning and filling was done in the same manner as for the DNMR samples.

III. RESULTS AND DISCUSSION

How substantially the confinement affects a liquid crystal bulk behavior strongly depends on the typical length scale of the confining material. As empirically extrapolated by combining results from a variety of confined studies, different behavior is found depending on how the porous material typical length scale compares with the nematic thermal correlation length ξ_N. At the $T_{N\text{-}I}$ transition, ξ_N is approximately 150 Å. Also, for confining length scales on the order of or smaller than ξ_N, one must consider interporous and/or intraporous interactions to model the host substrate.

A. Macroporous (1000 Å) confinement

As characterized from the DNMR spectral patterns, the orientational order of 8CB confined to the 1000 Å, macroporous glass exhibits confinement effects that are similar to those observed in previous studies that employed surface treated anopore and nuclepore membranes [31,34]. Examples of the observed spectra at several temperatures are shown in Fig. 1. Deep into the isotropic phase ($T-T_{N\text{-}I}{}^B \approx 13$ K), the DNMR spectrum consists of a single absorption peak ~0.12 kHz broader than that of bulk at the same temperature. This is an indication of surface induced order. The FWHM of this peak continuously grows with decreasing temperature to 0.50 kHz just above the transition (T_C). At T_C, determined as the temperature where a nematiclike quadrupolar splitting is first seen, the spectrum changes to one with a clear quadrupolar splitting ($\delta\nu=15$ kHz) coexisting with a prominent central absorption peak. Below T_C and with decreasing temperature, the FWHM of this central peak decreases slightly as plotted in Fig. 2. The T_C determined as described above is only slightly shifted downward from bulk (~0.1 K). The nematic to isotropic transition in the macroporous glass is a weakly first order transition with a broad two-phase region consisting of the coexistence of a nematic splitting with isotropiclike absorption peak.

The coexisting central peak is dependent on the thermal history of the sample. If the sample is cycled several times through T_C, and then slowly cooled through the transition at a rate $\leqslant 100$ mK/h, the intensity of the central peak becomes much smaller than that of the splitting peaks, as seen in Figs. 1(B) and 1(C). If the sample is rapidly cooled (quenched) below T_C from high temperatures, or removed from the

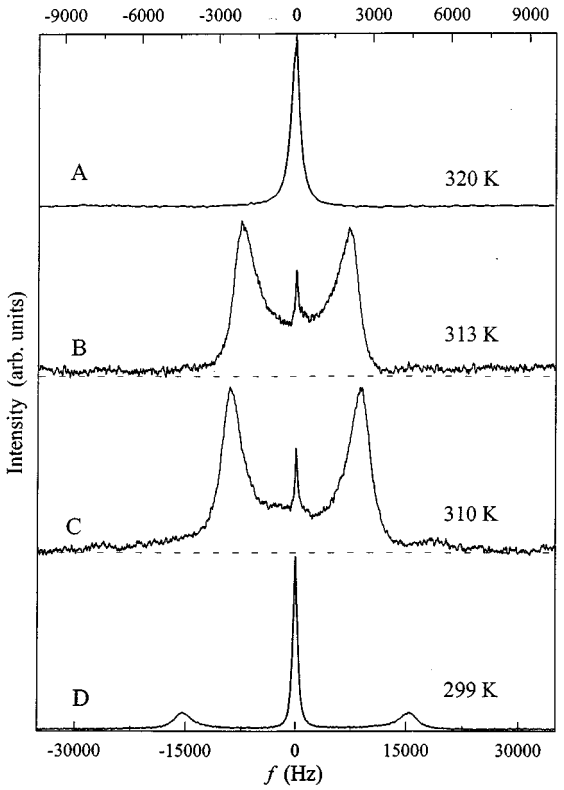

FIG. 1. DNMR spectrum of 8CB αd_2 confined to the 1000 Å macroporous glass at several temperatures. Spectra A uses the upper x axis, while spectra $B-D$ use the lower x axis. The powder–pattern spectra is mostly evident in spectra C.

NMR field and then replaced at the same temperature in the nematic phase, the intensity of the central peak is quite large compared to that of the splittings, as evidenced by Fig. 1(D). In both cases, its FWHM remains nearly the same. This indicates an annealing process that minimizes the amount of LC trapped in an isotropiclike state (probably defects at the

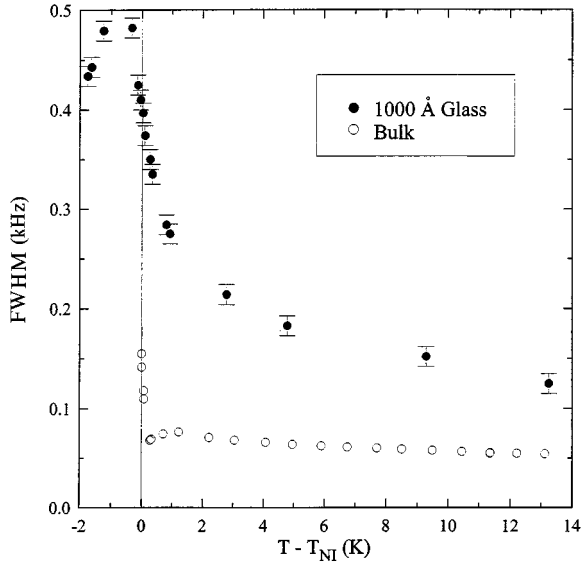

FIG. 2. Full width half maximum of the central absorption peak of 8CB-αd_2 confined to the 1000 Å macroporous glass as a function of temperature. Bulk 8CB is shown by the open circles.

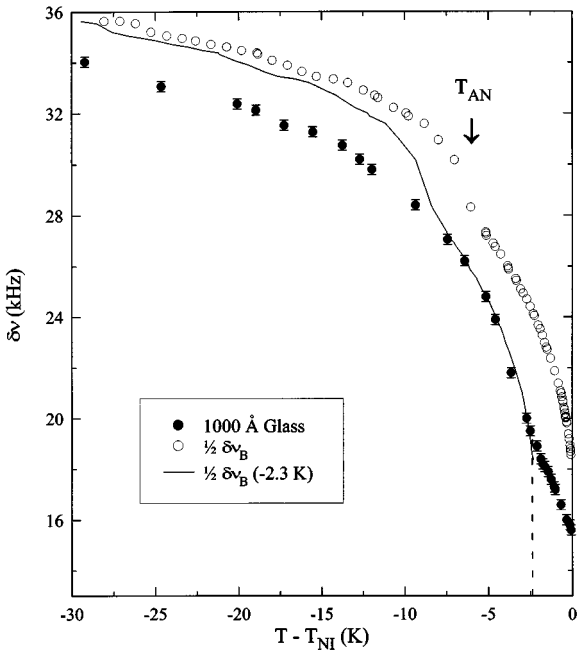

FIG. 3. The quadrupolar splitting of 8CB αd_2 below the N-I transition. The half splitting of bulk is shown by open circles. The solid line is one half of the bulk splitting shifted down 2.3 K.

pores centers) without completely ordering all LC molecules even at the lowest temperature studied ($T-T_C \approx -30$ K). This slow process suggests that it is difficult for the LC ordering to reach complete equilibrium. The presence of trapped defects appears to be a typical feature of liquid crystal systems in submicron size confinement [24,39].

We now compare the confined quadrupolar splitting with bulk's. Its magnitude $\delta\nu \cong 15$ kHz at T_C is approximately 3 kHz lower than $\frac{1}{2}\delta\nu_{\text{bulk}}$ at $T_{N\text{-}I}{}^B$. This is partly due to the disorder introduced by the random interconnected surfaces. The quadrupolar line shape is asymmetric, reminiscent of the upper part of a powder-pattern with the $\pi/2$ shoulders being too weak to observe, although the spectra shown in Fig. 1(C) is perfectly consistent with a powder pattern. Powder patterns, which are expected for liquid crystal samples confined to random interconnected geometries but are not easily obtained due to motional diffusion effects, indicate the presence of a random distribution of nematic domains. It is therefore appropriate to compare the confined splitting with 1/2 of that of a nematic sample fully aligned by an external magnetic field. On further cooling, $\delta\nu$ increases linearly until ~ 2.3 K below T_C where it then grows with a bulklike temperature dependence (similar curvature) with decreasing temperature, see Fig. 3. Curiously, the change in the temperature dependence of the confined nematic splitting coincides with the temperature at which the specific heat (see below) has a peak, i.e., the thermodynamically determined nematic to isotropic confined transition temperature.

The DNMR spectral pattern is completely independent of sample orientation with respect to the static NMR field, further supporting the idea of a random distribution of ordered domains (whose size cannot be inferred from these data) with a lower than bulk orientational order at all temperatures below T_C. The growth of $\delta\nu$ with decreasing temperature does not exhibit the anomalous increase associated with the

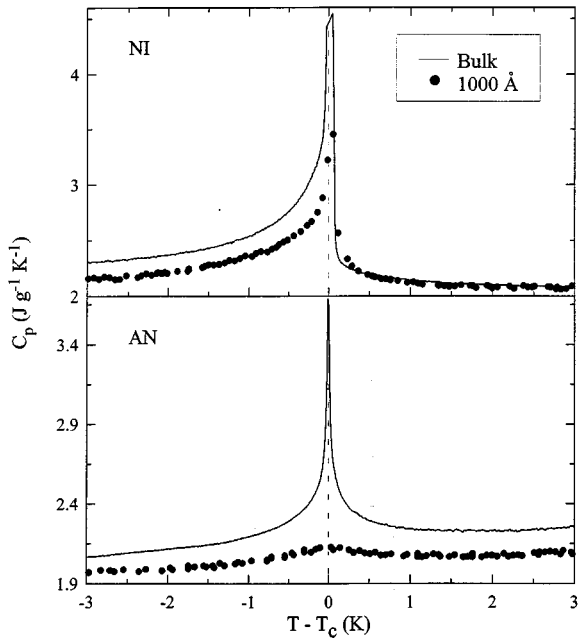

FIG. 4. Specific heat of 8CB confined to the 1000 Å macroporous glass at the *N-I* and *A-N* transition. Bulk transitions are indicated by the solid lines.

presence of smectic ordering which occurs at $T-T_{N\text{-}I}{}^{B}=7$ K for bulk (indicated by the arrow in Fig. 3). We are not interpreting this result to suggest that the smectic phase is not formed in the macroporous glass; there is in fact a suppressed smectic-*A* to nematic transition clearly detected by our calorimetry technique. Instead, we take this is as evidence for the decoupling of nematic and smectic order parameters due to the random confinement [40]. Long wavelength fluctuations, like nematic director fluctuations or smectic layers spatial fluctuations are suppressed to length scales comparable to the pore size. The nematic susceptibility is unaffected as the increase of nematic order with decreasing temperature is the same as bulk. Note that scattering experiments on other confined systems of similar pore size and geometry have unambiguously shown the formation of a shorter-ranged smectic phase [12,13].

The calorimetry results support the DNMR findings: a bulklike *N-I* C_p feature is seen at 311.91 K (with some rounding) while an extremely suppressed and broadened Sm-*A*–*N* C_p signature is observed at 304.41 K. The specific heat temperature dependence is plotted in Fig. 4. The calorimetry determined confined transition temperatures, T_C are shifted -2.05 and -2.61 K from the bulk *N-I* and Sm-*A*–*N* transitions, respectively. Consequently, the macroporous confinement appears to slightly increase the nematic range by ~ 0.5 K. The temperature of the confined *N-I* transition as measured by calorimetry is almost exactly the temperature where the bulklike temperature dependence of the DNMR splitting starts (see dashed line in Fig. 3). To within the accuracy of the absolute temperature obtained from the different thermometers employed in the two setups, there is no difference in $T_{N\text{-}I}$ for bulk 8CB. This suggests that T_C determined by DNMR is not a true reflection of the thermodynamic *N-I* phase transition, but it is a manifestation of the onset of bulklike orientational order in only that population of pores (within the macroporous glass) of size larger than the mean pore size. That there is a pore size distribution is known from transmission electron micrograph studies [41] and is a characteristic of most host substrates.

Comparing with other studies in confined geometries, from the data in Fig. 4 one can extract the magnitude of $\Delta C_p(\max)$ at both transitions after subtracting the background regular specific heat from the value at the transition, as well as the transition enthalpy, obtained from the area under the specific heat peak [37–38]. At the *N-I* transition $\Delta C_{pN\text{-}I}(\max)=1.34$ J/g K, a 45% suppression from bulk, and, $\Delta H_{N\text{-}I}=1.55$J/g, which is 30% lower than bulk. These values are not too different from those in 0.036 g/cm^3 aerogel. Similarly, at the *A-N* transition, we find that $\Delta C_{pA\text{-}N}(\max)=0.147\pm 0.01$ J/g K, which is the same as the value found in 0.08 g/cm^3 aerogel, which, although of a much higher porosity nearing 94.5%, has an average pore size ($\sim$700 Å) of similar order of magnitude to that of the macroporous glass. The *A-N* transition enthalpy is found to be 0.17 J/g, one-third of bulk, not unlike what is found for ~ 0.3 g/cm^3 aerogel. Further comparing with aerogel, the transition temperature in the macroporous glass is shifted ~ 1 K lower than that in the similarly sized aerogel; the shift is nearly the same as that found in the less porous 0.36 g/cm^3 aerogel [15]. From these results it is tempting to conclude that transition temperature shifts are mostly dictated by the host substrate porosity rather than the confining length. Most likely, the surface to volume ratio is what may dictate the changes in these thermodynamic quantities.

Since a smectic phase exists in the macroporous confinement, albeit possessing short-range order, the transition from a nematic phase appears to proceed as a glasslike process with a nearly complete suppression of pretransitional smectic fluctuations. This supports the earlier notion that the decoupling of the smectic and the nematic parameters for a narrow nematic range LC is accomplished through the suppression of quasi-long-range smectic and nematic ordering [40].

B. Microporous (100 Å) confinement

The DNMR and calorimetric results for the microporous confined 8CB sample are quite similar to those previously found for Vycor confined 8CB [24]. Over the 328–303 K range of the measurement, under this more restrictive confinement no quadrupolar splitting is observed. This is not surprising since the microporous glass and Vycor possess similar pore sizes (100 Å and 70 Å, respectively), similar porosity (25% to 28% for Vycor), and are formed using a similar manufacturing process [27].

The DNMR spectral patterns for 8CB confined to the 100 Å microporous glass at several temperatures are shown in Fig. 5. At all temperatures, the DNMR spectra consists of a single, nearly Lorentzian, absorption line which is much broader than that of bulk in the isotropic phase. The FWHM of this absorption peak continuously increases with decreasing temperature. From 328 to $\sim$308 K, its magnitude is slightly lower (by ~ 0.5 kHz) but its temperature dependence nearly identical to that found for 8CB confined to Vycor. The FWHM saturates at 308 K as seen in Fig. 6. Differences with respect to the Vycor results may be due to the absence of a clearly defined double Lorentzian line shape as observed in

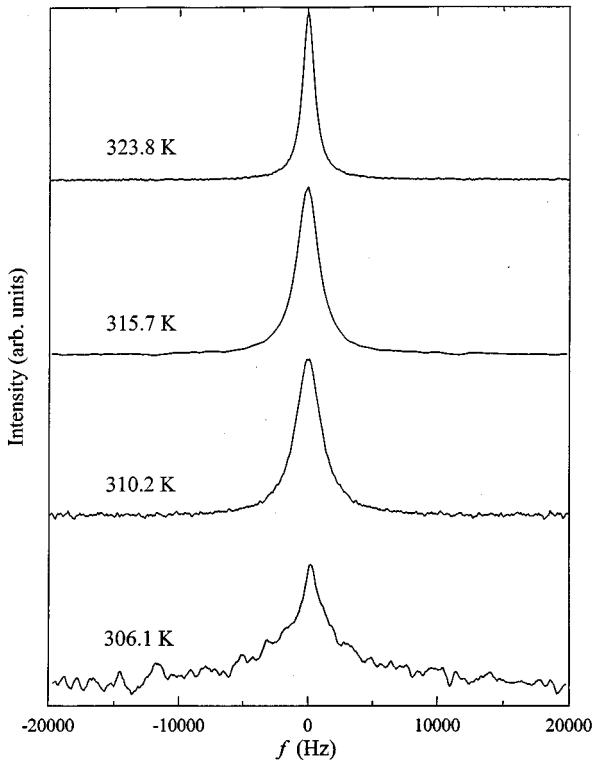

FIG. 5. DNMR spectra of 8CB αd_2 confined to 100 Å microporous glass at several temperatures.

Vycor that indicated the presence of defect cores in addition to the local order [24]. In addition, the effect of motional averaging, irrelevant in Vycor, may be of some influence here. The single-pore model that was valid for the 70 Å pores of Vycor, is not fully appropriate here and interporous or pore edge effect interactions must be included [26]. What is significant is that, given that the pore size is less than the nematic correlation length, these results imply that there is a

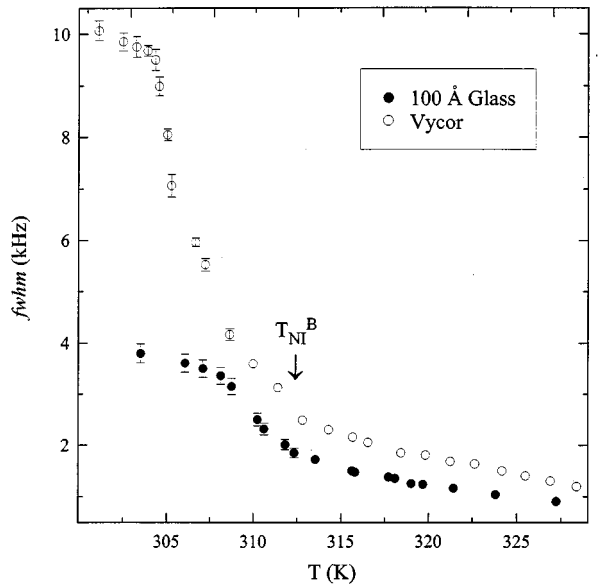

FIG. 6. Full width half maximum of 8CB αd_2 confined to the 100 Å microporous glass as a function of temperature. The open circles refer to results in Vycor from Ref. [23].

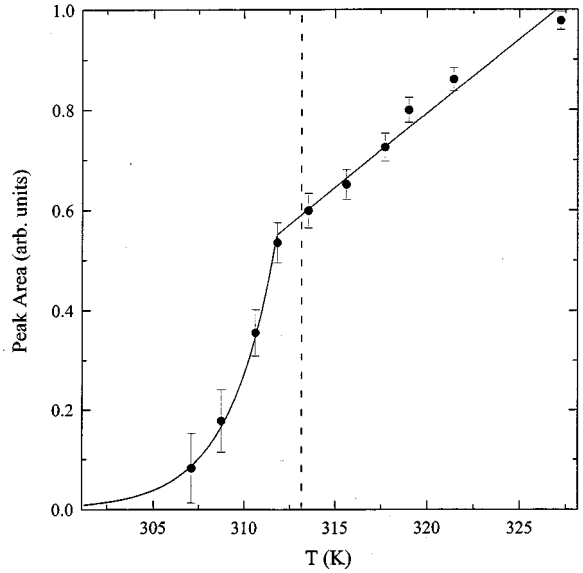

FIG. 7. Area under the single absorption peaks of microporous confined 8CB αd_2 as function of temperature. Note the deviation from linear behavior at $\sim$2 K below the bulk N-I transition shown as a dashed line. The solid line is a guide to the eye.

glasslike evolution of local orientational order which begins to saturate $\sim$5 K below $T_{N\text{-}I}{}^{B}$, 5 K sooner than the saturation in Vycor. Below this temperature, the relaxation time is too short to observe the now nearly 4 kHz broad absorption peak. This indicates that the confined LC is ''frozen'' into a glassy state.

We calculated the area under the DNMR absorption peak for equally averaged spectra [42] and its temperature dependence is shown in Fig. 7. The area under such peak is a measure of the number of molecules in that particular state. What is found is that the area decreases linearly with decreasing temperature until $\sim$2 K below $T_{N\text{-}I}{}^{B}$ where a more sudden and rapid decay to zero occurs. The temperature at which such a temperature dependence change occurs can be considered as the onset temperature of the orientational glass transition. The loss in the area under the intensity peak means that fewer molecules are contributing to the DNMR spectra, i.e., LC molecules become frozen with decreasing temperature. Clearly, the glasslike state hinders the diffusion of LC molecules preventing the established orientational order from representing the true equilibrium order. The LC molecules may become trapped in a metastable locally ordered state.

The calorimetric results plotted in Fig. 8 show no evidence of either a N-I or Sm-A–N transition over the entire temperature range studied. Instead, a stronger than bulk temperature dependent background C_P is observed at high temperature, with a slope of 0.018 J/g K^2. When extrapolated to lower temperatures, a rise in C_p rise is seen. This is likely the start of a very broad and suppressed bump which is evident in Fig. 8 and is the signature of a continuous evolution of local orientational order and its contribution to the specific heat.

IV. CONCLUSIONS

A study of the orientational order of 8CB confined to two randomly interconnected porous glasses having an order of

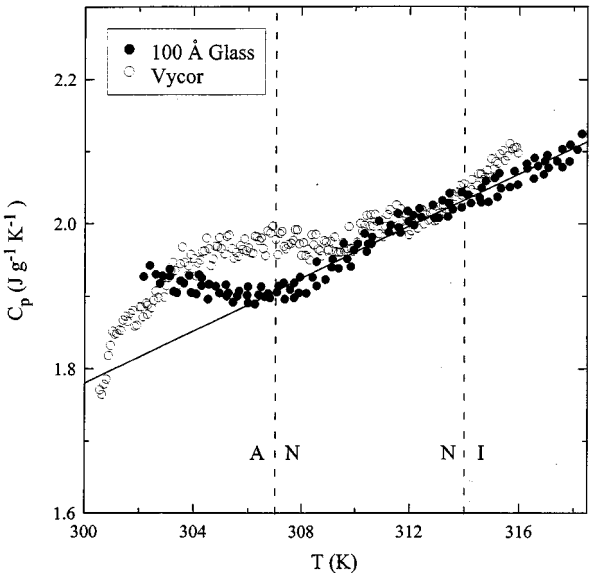

FIG. 8. The specific heat of microporous (λ) and Vycor (○) confined 8CB. Only the leading edge of the C_p ''bump'' observed in Vycor is seen in the 100 Å microporous glass. The vertical dashed lines indicate the bulk 8CB *N-I* and Sm-*A*–*N* transitions.

magnitude difference in mean pore size shows substantial modifications to the *N-I* and Sm-*A-N* transitions. Different effects are observed depending on whether the host material length scale is larger or smaller than the thermal nematic correlation length.

The microporous confinement generally confirms the results obtained from the similar Vycor confinement. The LC orders in a glasslike fashion evolving and increasing continuously with decreasing temperature. The area under the DNMR spectra peak linearly decreases with decreasing temperature until 2 K below the bulk *N-I* transition, where it rapidly decays until it is unobservable, indicating that LC molecules are frozen.

The macroporous confinement, where results have some similarity to those in silica aerogel, reveals interesting new features including a frozen ''isotropiclike'' component. This most likely arises from trapped defects (a common feature under confinement) and it is sensitive to the thermal history of the sample. This results from the severe constraints imposed by the porous network on the liquid crystal material and may indicate a metastable nonequilibrium nature of the ordering. The weakly first order nature of the *N-I* transition is retained while there is a broad two-phase coexistence region: nematic splitting and an isotropiclike absorption peak. The DNMR spectral pattern is powderlike, thus, the nematic phase is characterized by a random distribution of ordered domains.

The smectic phase although greatly modified is still present in the form of small domains. Pretransitional smectic fluctuations are suppressed by the rigid porous media as seen by the calorimetry studies. The nematic phase appears to be preferred by the surfaces as there is a 0.5 K increase in the nematic range. There is no drastic increase in the magnitude of the orientational order upon cooling into the smectic phase. This suggests that the smectic and nematic ordering are less coupled than in bulk and that the nematic susceptibility is unchanged. The decoupling of the order parameters may then arise from the slowing down or suppression of orientational fluctuations due to the random confining host.

ACKNOWLEDGMENTS

This research was supported by NSF-STC ALCOM Grant No. DMR 89-20147. Deuterated materials were provided by S. Keast and M. Neubert through the Resource Facility of ALCOM. One of us (F.M.A.) acknowledges the support from the U.S. Air Force Grant No. F49620-95-1-0520.

[1] D. F. Brewer, J. Low Temp. Phys. **3**, 205 (1970), and references therein.
[2] M. C. Goh, W. I. Goldburg, and C. M. Knobler, Phys. Rev. Lett. **58**, 1008 (1987).
[3] S. B. Dierker and P. Wiltzius, Phys. Rev. Lett. **58**, 1865 (1987); **66**, 1185 (1991); P. Wiltzius, S. B. Dierker, and B. S. Dennis, *ibid.* **62**, 804 (1989); S. B. Dierker, B. S. Dennis, and P. Wiltzius, J. Chem. Phys. **92**, 1320 (1992).
[4] F. Brochard and P. G. de Gennes, J. Phys. (France) Lett. **44**, 785 (1983).
[5] P. G. de Gennes, J. Phys. Chem. **88**, 6469 (1984).
[6] K. Binder and A. P. Young, Rev. Mod. Phys. **58**, 801 (1986), and references therein.
[7] X-l. Wu, W. I. Goldburg, M. X. Liu, and J. Z. Xue, Phys. Rev. Lett. **69**, 470 (1992).
[8] A. Maritan, M. Cieplak, T. Bellini, and J. R. Banavar, Phys. Rev. Lett. **72**, 4113 (1994); A. Maritan, M. Cieplak, and J. R. Banavar, in *Liquid Crystals in Complex Geometries Formed by Polymer and Porous Networks*, edited by G. P. Crawford and S. Zumer (Taylor and Francis, London, 1995), Chap. 22.
[9] Y. Y. Goldschmidt and A. Aharony, Phys. Rev. B **32**, 264 (1985).
[10] K. Uzelac, A. Hasmy, and R. Jullien, Phys. Rev. Lett. **74**, 422 (1995).
[11] D. J. Cleaver, S. Kralj, T. J. Sluckin, and M. P. Allen, in *Liquid Crystals in Complex Geometries Formed by Polymer and Porous Networks*, edited by G. P. Crawford and S. Zumer (Taylor and Francis, London, 1995), Chap. 21.
[12] T. Bellini *et al.*, Phys. Rev. Lett. **69**, 788 (1992).
[13] N. A. Clark *et al.*, Phys. Rev. Lett. **71**, 3505 (1993).
[14] T. Bellini, N. A. Clark, and D. W. Schaefer, Phys. Rev. Lett. **74**, 2740 (1995).
[15] L. Wu *et al.*, Phys. Rev. E **51**, 2157 (1995).
[16] A. J. Liu *et al.*, Phys. Rev. Lett. **65**, 1897 (1990).
[17] A. J. Liu and G. S. Grest, Phys. Rev. A **44**, R7894 (1991).
[18] L. Monette, A. J. Liu, and G. S. Grest, Phys. Rev. A **46**, 7664 (1992).
[19] F. Aliev, W. I. Goldburg, and X-l. Wu, Phys. Rev. E **47**, R3834 (1993).
[20] W. I. Goldburg, F. M. Aliev, and X-l. Wu, Physica A **213**, 61 (1995).
[21] M. Y. Lin *et al.*, Phys. Rev. Lett. **72**, 2207 (1994); G. Schwalb and F. W. Deeg, *ibid.* **74**, 1383 (1995).

[22] F. M. Aliev and M. N. Breganov, Zh. Éksp. Teor. Fiz. **95**, 122 (1989) [Sov. Phys. JETP **68**, 70 (1989)]; F. M. Aliev and K. S. Pozhivilko, Pis'ma Zh. Éksp. Teor. Fiz. **49**, 271 (1989) [JETP Lett. **49**, 308 (1989)].
[23] S. Kralj, G. Lahajnar, A. Zidansek, N. Vrbancic-Kopac, M. Vilfan, R. Blinc, and M. Kosec, Phys. Rev. E **48**, 340 (1993).
[24] G. S. Iannacchione *et al.*, Phys. Rev. Lett. **71**, 2595 (1993); G. S. Iannacchione *et al.*, Mol. Cryst. Liq. Cryst. **262**, 13 (1995); G. S. Iannacchione *et al.*, Phys. Rev. E **53**, 2402 (1996); G. Iannacchione and D. Finotello, in *Liquid Crystals in Complex Geometries Formed by Polymer and Porous Networks*, edited by G. P. Crawford and S. Zumer (Taylor and Francis, London, 1995), Chap. 16.
[25] Z. Zhang and A. Chakrabarti, Phys. Rev. E **52**, 4991 (1995).
[26] S. Tripathi, C. Rosenblatt, and F. M. Aliev, Phys. Rev. Lett. **72**, 2725 (1994).
[27] Corning Inc. trademark.
[28] P. Levitz, G. Ehret, S. K. Sinha, and J. M. Drake, J. Chem. Phys. **95**, 6151 (1991).
[29] J. Thoen, H. Marynissen, and W. Van Dael, Phys. Rev. A **26**, 2886 (1982).
[30] J. W. Doane, in *Magnetic Resonance of Phase Transitions*, edited by F. J. Owens, C. P. Poole, and H. A. Farach (Academic, New York, 1979).
[31] G. P. Crawford, R. Stannarius, and J. W. Doane, Phys. Rev. A **44**, 2558 (1991); D. W. Allender, G. P. Crawford, and J. W. Doane, Phys. Rev. Lett. **67**, 1442 (1991); R. J. Ondris-Crawford *et al.*, *ibid.* **70**, 194 (1993).
[32] A. Abragam, *The Principles of Nuclear Magnetism* (Clarendon, Oxford, 1962).
[33] P. G. de Gennes, *The Physics of Liquid Crystals* (Clarendon, Oxford, 1974).
[34] G. P. Crawford *et al.*, Phys. Rev. Lett. **66**, 72 (1991); **70**, 1838 (1993).
[35] P. Sullivan and G. Seidel, Phys. Rev. **173**, 679 (1969).
[36] C. W. Garland, in *Phase Transitions in Liquid Crystals*, edited by S. Martellucci and A. N. Chester (Plenum, New York, 1992), and references therein.
[37] G. S. Iannacchione and D. Finotello, Phys. Rev. Lett. **69**, 2094 (1992); Phys. Rev. E **50**, 4780 (1994), and references therein.
[38] D. Finotello and G. S. Iannacchione, Int. J. Mod. Phys. B **9**, 2247 (1995).
[39] G. S. Iannacchione *et al.*, Europhys. Lett. **36**, 425 (1996).
[40] S. Qian, G. S. Iannacchione, and D. Finotello, Phys. Rev. E **53**, R4291 (1996).
[41] F. M. Aliev (private communication).
[42] Equally averaged spectra means that only data from NMR spectral patterns acquired after an identical number of scans are used; this is because the intensity is arbitrary and depends on how long the data was accumulated.